The effect of column tilt on flow homogeneity and particle agitation in a liquid fluidized bed

Alicia Aguilar-Corona, Olivier Masbernat, Bernardo Figueroa-Espinoza, Roberto Zenit

The effect of column tilt on flow homogeneity and particle agitation in a liquid fluidized bed

A. Aguilar-Corona[a], O. Masbernat[b], B. Figueroa[c], R. Zenit[d,*]

[a] Facultad de Ingeniería Mecánica, Universidad Michoacana de San Nicolás de Hidalgo, Francisco J. Mujica s/n C.P. 58030, Morelia-Michoacán, México
[b] Laboratoire de Génie Chimique, Université de Toulouse, CNRS/INPT-UPS, 4, allée Emile Monso BP 44362, 31030 Toulouse Cedex 4, France
[c] Laboratorio de Ingeniería y Procesos Costeros, Instituto de Ingeniería, Universidad Nacional Autónoma de México, Puerto de Abrigo S/N, Sisal, Yucatán 97355, México
[d] Instituto de Investigaciones en Materiales, Universidad Nacional Autónoma de México, Apdo, Postal 70-360, México D.F., 04510, México

A B S T R A C T

The motion of particles in a solid-liquid fluidized bed was experimentally studied by video tracking of marked particles in a matched refractive index medium. In this study, two fluidized states are compared, one carefully aligned in the vertical direction ensuring a homogeneous fluidisation and another one with a non-homogeneous fluidisation regime that results from a slight tilt of the fluidisation column of 0.3° with respect to the vertical. As a result of the misalignment, large recirculation loops develop within the bed in a well-defined spatial region. It is found that in that range of solid fraction (between 0.3 and 0.4), the inhomogeneous motion of the particles leads to significant differences in velocity fluctuations as well as in self-diffusion coefficient of the particles in the vertical direction, whereas the fluidisation height remains unaffected. At lower (less than 0.2) or higher (higher than 0.5) concentration, particle agitation characteristics are almost unchanged in the vertical direction.

Keywords:
Agitation
Liquid fluidized bed
Homogenization
Solid fraction
Column tilt

1. Introduction

The study of liquid fluidisation is significant from both theoretical and practical viewpoints. It allows for the experimental verification of two-fluid modelling concepts in gravity driven solid-liquid flows, where the slip velocity is of the same order of magnitude as that of the continuous phase and where solid phase agitation is induced by collisional and hydrodynamic interactions (the contribution due to the continuous phase turbulence being negligible compared to the aforementioned interactions). Even if a liquid fluidized bed does not exhibit chaotic mixing or sharp regime transitions (as in the case of bubbly flows), a state of homogeneous fluidisation is seldom observed.

The concept of a homogeneous bed is usually referred to the appearance of solid fraction fluctuations which are observable at macroscopic scale, characterized by particle-free regions or voids of different shapes: depending on the fluidisation conditions, a fluidized bed can destabilize in the sense of the appearance of one-dimensional traveling waves (ODTW) (Anderson and Jackson, 1969) which may later develop into two-dimensional structures and transitions to other flow regimes such as the formation of bubbles, and structures that remind oblique waves (Didwania and Homsy, 1981; Duru and Guazzelli, 2002; El-Kaissy and Homsy, 1976; Homsy et al., 1980). There are many investigations that try to map such transitions through experimental, theoretical and numerical simulation in the literature, the reader may refer to (Di Felice, 1995; Homsy, 1998; Sundaresan, 2003) for a more comprehensive review.

In this work we study homogeneity from a different viewpoint; the column is (or is not) homogeneous in terms of the absence of large scale recirculation and the break of symmetry of the flow velocity field in terms of some statistical parameters that characterizes it in space or in time (Gordon, 1963; Handley et al., 1966). The homogenization concept is not easily defined because low frequency motion is always present due to confinement (Buyevich, 1994). This effect is evident when the particle motion is studied for relatively long time, so the particles have enough time to traverse many times the column length and diameter. Two dimensional analyses often turn out to be insufficient because the system is not guaranteed to be symmetric and the formation of low frequency structures may not be observed from a given observation direction. This is why a full three dimensional analysis is fundamentally important to characterize a liquid fluidisation system. It also allows for direct comparisons with numerical results.

The effect of inclination on a fluidized bed is of particular relevance in the context of this study. It has been investigated from several viewpoints in the literature: for gas-solid fluidisa-

* Corresponding author.
E-mail address: zenit@unam.mx (R. Zenit).

tion one can find many previous relevant works: in particular, in Yamazaki et al. (1989) the minimum fluidisation velocity for inclined columns was studied. The authors observed three distinct flow regimes (fixed bed, partially fluidized and completely fluidized), and noted the effect of column inclination on the corresponding regime transitions. Yakubov et al. (2005) studied the effect of inclination of a liquid-solid fluidized bed on several working parameters such as critical flow rate, bed height and dynamic pressure drop. They observed a pattern of concentration waves (for the effect of inclination in the case of cohesive powders, see (Valverde et al., 2008)). Numerical investigations have also been carried out on the subject; in Chaikittisilp et al. (2006) Discrete Element Simulations (DEM) were used to study gas-solid two-phase flow, in order to investigate the mixing behavior of the solid phase in inclined fluidized beds. A large scale recirculation pattern was observed. Low concentration bubbles tend to move upwards along the uppermost wall, contrary to the particles that moved downward, closer to the wall below it, enhancing back mixing. This behavior has also been observed experimentally in gas-liquid bubbly flows, due to buoyancy, for very small tilt angles (Zenit et al., 2004).

For liquid-solid fluidized beds, little attention has been paid to the effect of inclination on the column homogeneity. Hudson et al. (1996) used salt tracer measurements to conclude that fluidized bed inclination strongly affects the column hydrodynamics. Moreover, in Del Pozo et al. (1992) it was shown that a small tilt angle of 1.5° on a three-phase fluidized bed affects the particle-liquid mass and heat transfer coefficients significantly. Other important aspect in the complex interaction between solid and liquid phases is the effect of the inclination angle on mixing and diffusion, as a function of the relevant parameters such as the Reynolds number, Stokes number, and particle-column width (or height) ratio. Several studies have been devoted to the diffusion in a liquid-solid fluidized bed (Al-Dibouni and Garside, 1979; Carlos C. and Richardson J., 1968; Dorgelo et al., 1985; Juma and Richardson, 1983; Kennedy S. and Bretton R., 1966; Van Der Meer et al., 1984; Willus, 1970). Two trends can be identified in the literature concerning diffusion: firstly, with respect to solid concentration, and secondly, with respect to the particle-to-column diameter ratio. In some investigations (Carlos C. and Richardson J., 1968; Willus, 1970; Dorgelo et al., 1985) it is found that the diffusion coefficient decreases as solid fraction increases. On the other hand, other studies from the literature (Kang et al., 1990; Yutani et al., 1982) found a small peak on the auto-diffusion coefficient as the solid fraction concentration increases. Concerning the particle size ratio, the experiments showed that diffusion decreases as the particle size ratio increases. Those experiments were carried out for different flow regimes comprising superficial Reynolds numbers of O(10–1000) and two-phase Stokes numbers of O(1–10). Although there are many investigations devoted to the effect of inclination on liquid-solid fluidized beds, none of the aforementioned works remarked the high sensitivity of the fluidized bed characteristics to a small inclination; most of those studies comprised ranges of inclination between horizontal to vertical, but incremented the tilt in large steps, ignoring the effects of very small inclination angles.

This work is devoted to study the effect of a small tilt of the fluidisation column (0.3° with the vertical), compared to a vertically aligned column. Low frequency structures are detected and their effect on the dispersed phase velocity is assessed through the analysis of: a) The particle trajectories, b) The spatial distribution of the vertical speed, c) The particle velocity variances and d) The diffusion coefficient. The technique used to calculate the mean velocity and agitation (velocity variances) along the three directions is similar to that used in Handley et al. (1966) and Carlos and Richardson (1968) and later revisited in Buyevich (1994), Willus (1970) and Latif and Richardson (1972), who used a Lagrangian tracking of a colored particle in the bulk of a transparent bed. More recently a similar particle tracking technique was used but in a carefully controlled optically matched system (Aguilar, 2008; Aguilar Corona et al., 2011; Hassan and Dominguez-Ontiveros, 2008). A camera with high resolution was used (both in time and space), which allowed for the determination of detailed information about the particle phase motion within the fluidized bed.

2. Experimental set-up

The experimental device is shown schematically in Fig. 1. The fluidisation section is composed of a 60 cm high cylindrical glass column of 8 cm inner diameter. A flow homogenizer, consisting of a fixed bed of packed beads covered by synthetic foam layers, is mounted at the bottom of the column to ensure a homogeneous flow entry. The flow temperature is maintained at 20 °C by a controlled heat exchanger. Two particular cases were studied during this work: 1) A vertically aligned column and 2) A tilted column, forming an angle in the (y,z) plane of 0.3° with respect to the vertical axis z. The reference frame is shown in Fig. 2.

2.1. Particles and fluid

Calibrated 3 mm pyrex beads were fluidized by a concentrated aqueous solution of Potassium Thiocyanate (KSCN, 64% w/w). At 20 °C, the fluid and the particles and fluid have the same refractive index (∼1.474), so that a tagged (colored) particle could be tracked individually in a nearly transparent suspension (Aguilar-Corona et al., 2011). Particle and fluid properties are reported in Table 1. The particle Stokes and Reynolds numbers, based on the terminal (sedimentation) velocity, are $St = 4.8$ and $Re = 160$, respectively.

2.2. Particle tracking technique

The analysis of particle motion in the fluidized bed was performed by means of high speed 3-D trajectography. The fluidisation column is equipped with an external glass box filled with the aqueous phase in order to reduce optical distortion (see Fig. 2). A mirror oriented at 45° to the side of the box allowed for the observation of the particle path in three dimensions, providing an additional side view. A Photron APX camera equipped with a CMOS sensor was used to record the front ((x,z) plane) and the side view from the mirror ((y,z) plane) in a single frame (512 pix × 1024 pix). Images were recorded over periods of 204 seconds, starting after the stationary regime had been reached. Taking a characteristic particle velocity of 3 cm/s (from the standard deviation of the particle velocity of a typical experiment), this total time would represent more than 70 times the time a particle would take to travel one column diameter. The average residence time (the average of the time it takes to a particle to travel one column height) for the aligned case was 6 seconds, while the corresponding value for the tilted case was 4.5 s, so one can expect the average absolute speed to increase with inclination. A black colored particle was introduced in the bed and its trajectory was recorded at 60 frames per second (fps).

Fig. 3 shows both front (x-z plane) and side (y-z plane) views as captured by the camera, for solid fractions of $\langle\alpha_p\rangle = 0.50$ and $\langle\alpha_p\rangle = 0.14$ (sub-figures (a) and (b), respectively). All the experiments were carried out with a particle size of $d_p = 3$ mm. The black line between the images is just the space between the front wall and the mirror, which was masked in order to avoid a confusing view of the adjacent wall of the column. The image from the mirror had a slightly different scale due to the optical paths between the (direct) front view and that coming from the mirror, so each plane had its corresponding (horizontal and vertical) scale factor in

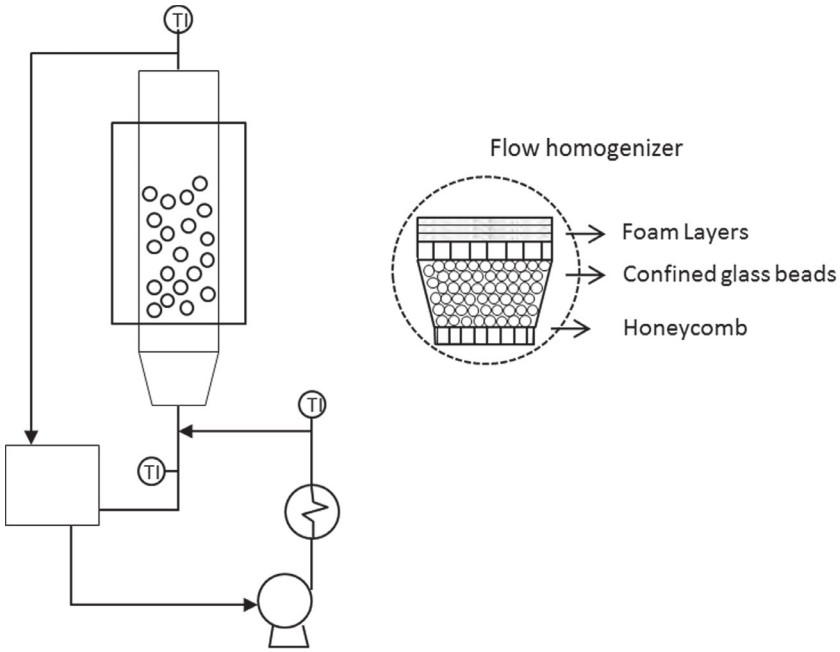

Fig. 1. Scheme of the experimental set-up and the entry section.

Table 1.
Fluid and particle properties at 20 °C.

Pyrex beads	$d_p = 3$mm	$\rho_p = 2230$ kgm^{-3}	$n_D = 1.474$
KSCN solution 64% *w/w*	$\mu_f = 3.8 \times 10^{-3}$ Pa s	$\rho_f = 1400$kgm^{-3}	$n_D = 1.474$

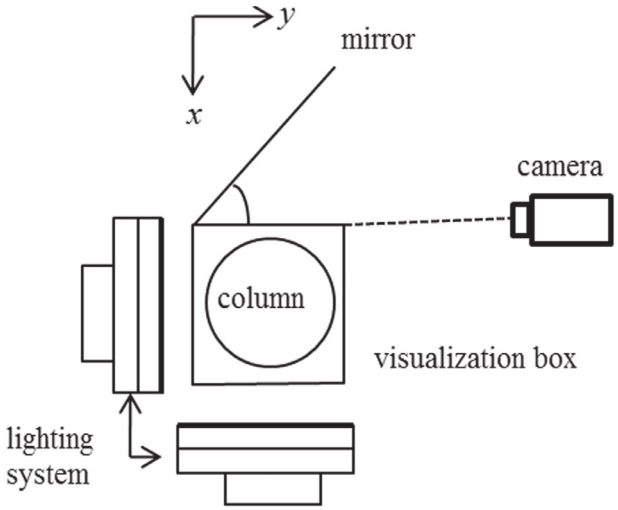

Fig. 2. Top view scheme of the trajectography 3D system.

order to obtain the actual position in centimeters after image digital processing. Note that the colored particle is clearly discernible even when it is located deep inside the bulk of the column (even for large solid fraction). It can be seen from the Figure (d.1 and d.2) that the particle diameter occupies approximately 13 to 15 pixels.

3. Results

3.1. Global solid fraction

The initial volume of particles in the fixed bed corresponds to an initial height h_0 of 9.5 cm, slightly larger than the column diameter. The maximum compactness concentration $\langle\alpha_c\rangle$ was estimated to be 0.56, corresponding to a random packing. Even though the system is optically homogeneous, beads interfaces are still detectable; a careful observation of the images allowed for the determination of the maximum height reached by the particles h_b for each solid fraction. The mean solid fraction was obtained as:

$$\langle\alpha_p\rangle = \langle\alpha_c\rangle \frac{h_0}{h_b}. \quad (1)$$

The bracket symbol represents the time and space averaging over the bed volume of the local instantaneous solid fraction. It was observed that the h_b fluctuations decreased as the solid fraction increased, with a relative error of less than 5% in all cases. In this work, five fluidisation velocities were tested (0.095, 0.078, 0.053, 0.038 and 0.02 m/s) corresponding to global solid fractions $\langle\alpha_p\rangle$ of 0.14, 0.2, 0.3, 0.4 and 0.5 respectively. For the homogeneous case, the fluidisation velocity U_F (fluid velocity in empty column) was found to be a decreasing power law of void fraction:

$$U_F = 0.145(1 - \langle\alpha_p\rangle)^{2.78} \quad (2)$$

where the prefactor is close to the particle terminal velocity (0.135 m/s) and the exponent value, $n = 2.78$, is close to that predicted by Richardson-Zaki's correlation ($n = 4.4\ Re_t^{-0.1} = 2.67$).

A first visual observation indicates that the slight tilt did not have any measurable effect on the bed expansion, so for each fluidisation velocity studied, the global solid fraction remained unchanged in both homogeneous (vertically aligned) and inhomogeneous (tilted column) cases. This observation is consistent with the averaged momentum balance in the bed volume. At first order, the effect of fluid and particle friction at the wall being neglected, this balance reduces to equilibrium between buoyancy force term and drag force term based upon mean slip velocity, i.e. the mean liquid velocity. The average solid fraction, or equivalently the bed height, results from this balance. However, when spatially averag-

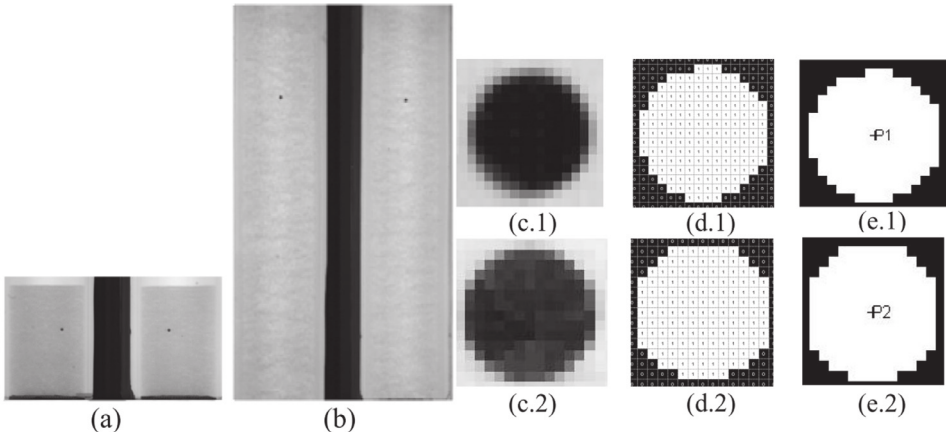

Fig. 3. Raw images as captured by the camera: a) Large solid fraction: $<\alpha_p>=0.5$; to the left of the black division: front view (x-z plane). To the right of the division is the lateral view (y-z plane). b) Moderate solid fraction: $<\alpha_p>=0.14$ (same views as in (a)); c) Particle close-up; c.1) front view and c.2) side view; d) Binarized particle image. (d.1) front view and (d.2) side view; e) Centroid detection: (e.1) and (e.2) correspond to front view and mirror image, respectively.

ing the local two-phase momentum transport equation, two contributions arising from the fluctuating motion of the particles and the fluid need also to be considered: one is the non-linear drag force term through the velocity fluctuations and the second is the cross-correlation between the spatial fluctuations of solid fraction and pressure gradient in the bed. It can be shown that in all range of fluidisation velocities, the first contribution is always larger than the second one, which roughly scales as few percent of the mean drag term. As a consequence, in a homogeneous liquid fluidized bed, the bed height is weakly dependent upon phase agitation. In a reference frame where the axial direction is the axis of the column, the buoyancy force component is $\Delta\rho g\cos\theta$ where is the angle with the vertical (0.3°), so the relative variation of this term is of order of 10^{-5} and can be neglected. Therefore, tilting the column a small angle (0.3°) will not modify the bed height, even though this perturbation induces important flow inhomogeneities and significant variations of particle fluctuations, as discussed in the next sections.

3.2. Particle trajectories

Fig. 4 shows particle trajectories recorded at three different concentrations. The left panel of the figure shows the trajectories projection in the horizontal (x,y) plane of the column, while the right panel displays the projections in the vertical (x,z) plane. For moderate solid fractions ($<\alpha_p>=0.14$ and $<\alpha_p>=0.20$) the particle path was observed to span the whole bed volume without exhibiting clear coherent structures. At larger solid fractions, a toroidal structure was observed in the lower part of the bed, along with a corresponding increase of the low frequency fluctuations. The origin of this steady structure has not been clarified yet. One possible explanation could be that due to a wall effect: a slip velocity difference between the middle and the near-wall region develops in the entry section, resulting in a solid fraction horizontal gradient. This solid fraction gradient would then induce a horizontal pressure gradient that would generate this recirculation pattern. But such a mechanism needs a more in depth analysis, which is beyond the scope of this paper.

Fig. 5 shows a comparison between the particle trajectories of the vertical column and the tilted one, corresponding to the (x,z), (y,z) and (x,y) planes for a solid fraction of $<\alpha_p>=0.30$. In the tilted column case (for that concentration) a well-defined recirculation loop in the (y,z) plane was observed, where the tracer particle trajectory forms an annulus. For the same case, in the (x,z) plane the particle path spans across the whole column volume without any preferential motion of the dispersed phase. Inclination induces a buoyancy force component normal to the wall; however, the counterbalance of this force cannot be readily identified if there are no significant changes in concentration or velocity. Therefore, this small imbalance may generate a radial drift velocity at the scale of each particle. Now as this drift velocity is likely to induce a radial concentration gradient, collective effects (such as a radial apparent density gradient) are probably driving the recirculating motion at the bed scale that is observed on trajectory patterns (similar in that sense to the so-called Boycott effect).

3.3. Test of homogeneity

In order to characterize fluidisation homogeneity, for each mean fluidisation velocity studied, the spatial distribution of upward and downward particle motion was analyzed in four distinct cross sections S_i, ($i=1$ to 4) regularly distributed along the bed height ($0\le z_{S1}\le 0.25h_b$; $0.25h_b<z_{S2}\le 0.50h_b$; $0.50h_b<z_{S3}\le 0.75h_b$; $0.75h_b<z_{S4}\le h_b$), as schematized in Fig. 6.

Fig. 7 shows the velocity sign distributions following particles trajectories in each test section S_i, for a global solid fraction of 0.3. Both aligned (left column) and tilted (right column) cases are displayed in this figure. The direction of the motion is indicated with a cross symbol if the particle moved downwards or a circle if it moved upwards as it crossed the plane S_i. For the vertically aligned case the signature of an axisymmetric toroidal motion at the lowermost part of the bed can be identified, with a preferential concentration of ascending velocities at the center of the bed cross-section, and descending velocity in the near-wall region. In the uppermost section, the distribution appears homogeneous over the cross-section. For the tilted case there is a preferential motion in all test sections, which consists of a large-scale recirculation over the whole bed volume, where the particle tends to rise in one half-section in Fig. 7-(ii), and to descend in the other one. Note that this motion is quite parallel to the (y,z) plane as expected. These plots clearly demonstrate the effect of the tilt on the particle motion in the fluidized bed.

In order to quantify homogeneity in the cylindrical geometry, the (circular) cross-section S_i was divided into 12 sectors of 30° each in the angular direction. The probability of particle crossing in a particular sector j with ascending vertical motion was calculated as:

$$\varphi_{up,j}=\frac{n_{up,j}}{n_j} \tag{4}$$

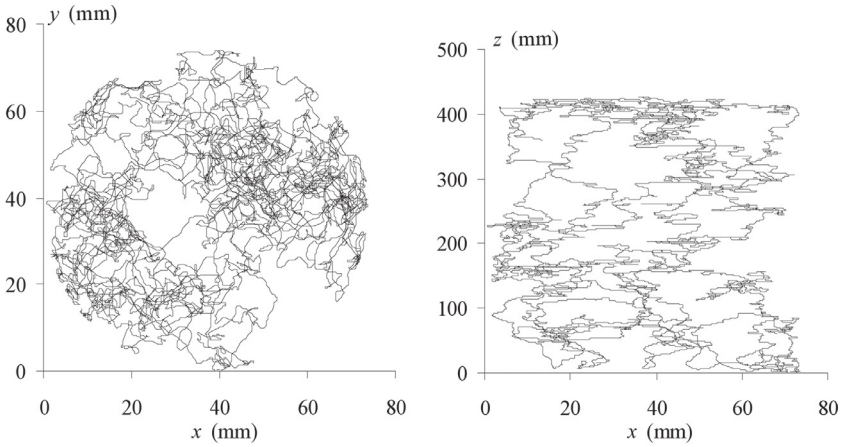

(a) $<\alpha_p>$ =0.14

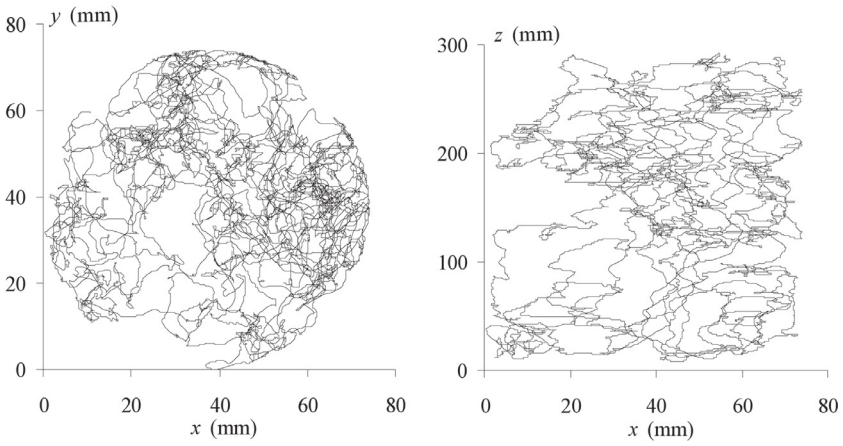

(b) $<\alpha_p>$ =0.20

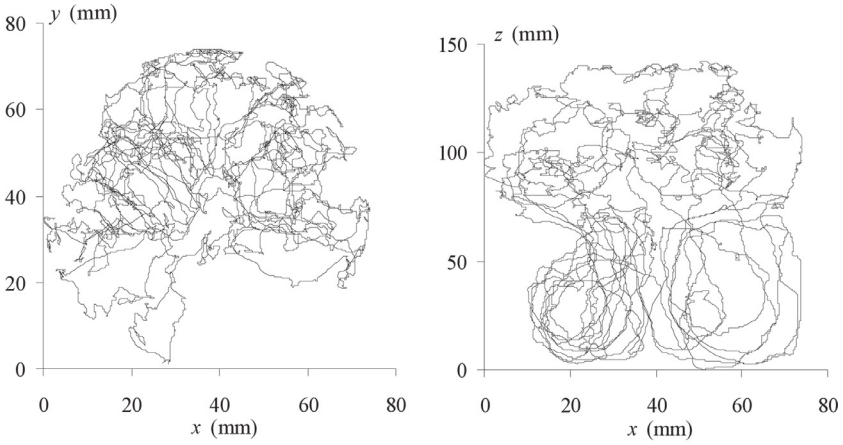

(c) $<\alpha_p>$ =0.40

Fig. 4. Particle trajectories projection for the vertically aligned case at a) $<\alpha_p>=0.14$, b) $<\alpha_p>=0.20$ and c) $<\alpha_p>=0.40$: left and right columns correspond to the horizontal (x,y) and vertical (x,z) planes, respectively.

with n_j the total number of particle crossing in sector j. This probability is mutually exclusive with respect to its counterpart (downwards crossing) $\varphi_{down,j}$. A perfectly homogeneous column would attain a value of $\varphi_{up,\ j}=0.5$ for all sectors ($j=1$ to 12 in this case), which in a polar representations would give a circle of radius ½. Figs. 8 and 9 show this type of representation, for the case of the aligned and tilted columns, respectively. The dotted circle has radius $r=0.5$, for comparison.

Fig. 8 shows an angular distribution close to homogeneous for S_4, while there seems to be more downwards moving particles for S_1. There are small deviations from ½ for S_2 and S_3. Fig. 9 shows the distribution $\varphi_{up,j}$ for the tilted column. It can be observed that

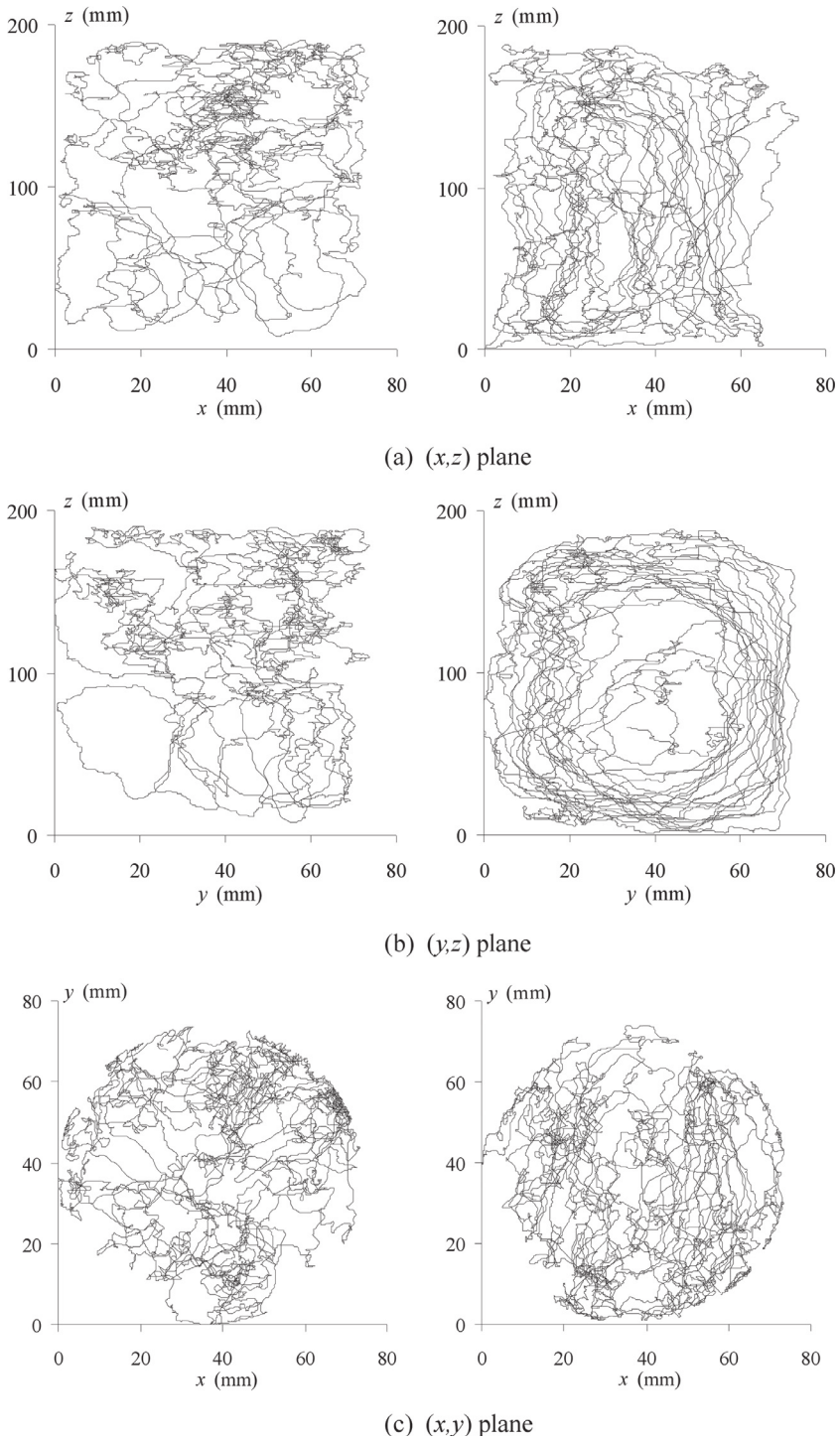

Fig. 5. Particle trajectories projection at $< \alpha_p > = 0.30$ in a) (x,z) plane; b) (y,z) plane; c) (x,y) plane. Left and right columns correspond to the aligned and tilted cases, respectively.

the distribution is close to the center for the first three sectors, and more homogeneous in S_4. However there is still a trend, showing $\varphi_{up,j} > 0.5$ in the second quadrant, with values below 0.5 for the third and fourth quadrants (values closer to one mean that more particles move upwards, consistent with Fig. 7(ii)). If the particles were less dense than the liquid, the particles would descend (in average) on the first and third quadrants.

Another way to represent Figs. 8 and 9 is to plot the angular standard deviation of $\varphi_{up,j}$ in each sector for the vertical and tilted cases. This quantity is plotted along bed height in Fig. 10 for the vertical and tilted cases. An increase by a factor close to 3 or 4 of the reference values in the vertical case can be observed in the tilted case. Note there is a correspondence between the four points in Figs. 10 and 9 for S_1, S_2, S_3 and S_4. The more heterogeneous distribution of the vertical velocity component was observed at S_2 and S_3, where the value of $\varphi_{up,j}$ is very small in the 3rd and 4th quadrants, indicating downwards vertical motion in these quadrants. The most homogeneous section was S_4, consistent with Fig. 9, where $\varphi_{up,j}$ is close to 0.5 in the 3rd and 4th quadrants. Note that these data is for $<\alpha_p> = 0.3$.

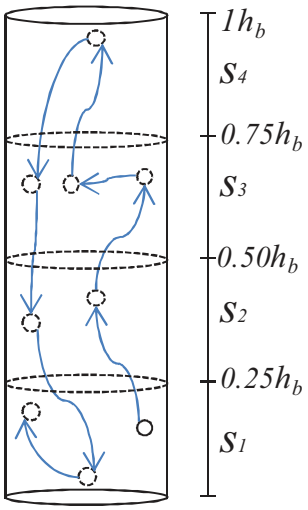

Fig. 6. Bed test cross sections S_1, S_2, S_3 and S_4.

Consequences of column tilt-induced flow inhomogeneities upon particle agitation are examined in what follows, by computing the particles velocity variance and self-diffusion coefficient and comparing their intensities with those of the aligned case.

3.4. Effect of column tilting on particle velocity variance

The variance of the ith particle velocity component in the bed is computed as:

$$\left\langle u'^2_{pi} \right\rangle = \left\langle \left(u_{pi}(t, x(t)) - \langle u_{pi} \rangle \right)^2 \right\rangle \tag{6}$$

where $u_{pi}(t,\mathbf{x}(t))$ is the instantaneous velocity i-component following particle trajectory $\mathbf{x}(t)$, and the bracket symbol denotes here the average of particle velocity ith-component over all trajectories (equivalent to an ensemble average operator). Note that $\langle u_{pi} \rangle$ is close to zero, the average particle velocity in the bed being zero for a steady fluidized bed (so u'_{pi} is very close to u_{pi}). In Fig. 11, the variance of each velocity component is reported as a function of global solid fraction, in both homogeneous (vertically aligned) and inhomogeneous (tilted) cases. In both cases, particle agitation is strongly anisotropic as expected in gravity-driven two-phase flows.

In the homogeneous case, the axial component of particle velocity variance (z-component) being about 2 times larger than the components in the horizontal plane (x,y) for all concentrations. Particle velocity variance is a continuously decreasing function in the range of concentration investigated [0.14–0.5], with a probable maximum lying in the range [0–0.14].

In the non-homogeneous case, the evolution of the axial velocity variance is quite different compared to the homogeneous case, mainly in the range of solid fraction [0.3–0.4]. At the lowest concentration ($<\alpha_p>=0.14$), the axial velocity variance is smaller than in the homogeneous case, then abruptly increases up to a maximum at $<\alpha_p>=0.3$, then strongly decreases between $<\alpha_p>=0.3$ and 0.5. This evolution results from the progressive development of the large-scale loop induced by the column tilt as the particle concentration increases. In the horizontal plane, particle velocity variance is a continuous decreasing function of solid fraction, slightly below the homogeneous case values in the range [0.14–0.3] with a similar behavior at higher concentration ($<\alpha_p>=0.5$).

Table 2 reports the relative difference between the particle velocity component variances for the homogeneous (noted $\langle u'^2_{pi} \rangle_H$) and non-homogenous (noted $\langle u'^2_{pi} \rangle_H$) fluidisation cases, measured at five different global solid fractions $\langle \alpha_p \rangle$, and defined as:

Table 2.
Relative difference δu_{p_i} of $\langle u'^2_{pi} \rangle_H$ between homogeneous and inhomogeneous cases.

$<\alpha_p>$	δu_x	δu_y	δu_z
0.14	0.12	0.22	0.15
0.2	0.10	0.16	−0.015
0.3	0.20	0.08	−0.59
0.4	0.18	−0.04	−0.6
0.5	−0.08	−0.1	0.09

$$\delta u_{pi} = 1 - \frac{\left\langle u'^2_{pi} \right\rangle_{nH}}{\left\langle u'^2_{pi} \right\rangle_H} \tag{7}$$

Positive values of δu_{pi} indicate that the ith-component velocity variance in the non-homogeneous case is smaller than that of the homogeneous case whereas negative values of δu_{pi} reveal the opposite trend. Note that in the homogeneous case, the velocity variance in x and y-direction should be equal. The relative difference between these values is in average of the order of 0.05 for all concentrations, so the relative difference between non-homogeneous and homogeneous case is considered as significant when its value exceeds 0.1. Large negative values are observed for the axial components of the variance, reaching $\delta u_{pz}=0.6$ at $<\alpha_p>=0.3$ and 0.4, which confirms the predominance of large-scale motions in that range of concentration. In the horizontal (x,y) plane, the relative difference is smaller than in the homogeneous case when $<\alpha_p>\leq 0.3$. At the highest concentration ($<\alpha_p>=0.5$), the difference becomes slightly negative.

If, in the non-homogeneous case, particles are globally accelerated in the vertical direction by a large scale motion induced by collective effects, then it can be understood that velocity fluctuations in the transverse directions will diminish in the ascendant and descendant parts of the loop, and increase in the horizontal part. In average, the transverse component variance will decrease, probably because the weight of the ascending and descending parts is stronger than that in the horizontal plane. At high concentration (0.5), the sign of the criterion is reversed, likely due to an aspect ratio effect (in this case, the height of the bed is indeed close to the column diameter). In the range [0.14, 0.2], the concentration seem to be too small to induce a large recirculation loop in the bed, but a non-zero transverse component of buoyancy still exists and is able to damp in the horizontal plane the fluctuating motion of particles produced by the mean drag force.

3.4. Effect of column tilting on particle diffusion coefficient

Particle diffusion coefficient is determined from the computation of Lagrangian velocity autocorrelation coefficient, defined for each velocity component u_{pi} as:

$$R_{ii}(t) = \frac{\left\langle u_{pi}(\tau) u_{pi}(\tau + t) \right\rangle}{\left\langle u^2_{pi}(\tau) \right\rangle} \tag{8}$$

In the range of global solid fraction investigated, particle Lagrangian velocity decorrelates within a time interval smaller than 4 seconds, as illustrated in Fig. 12. The curves in such figure can be fitted to a decaying exponential of the form $R_{ii}(t)=\exp(-bt)$; The fitted curve has an exponent $b=5.541\ s^{-1}$ (with R square of 0.990) for the z component, while for the x and y components it gives $b=11.15\ s^{-1}$ (with R square of 0.987). The time integration of the autocorrelation coefficient over this time interval gives the Lagrangian integral time scale for each component:

$$T^L_{ii} = \int_0^{T_{max}} R_{ii}(t)dt \tag{9}$$

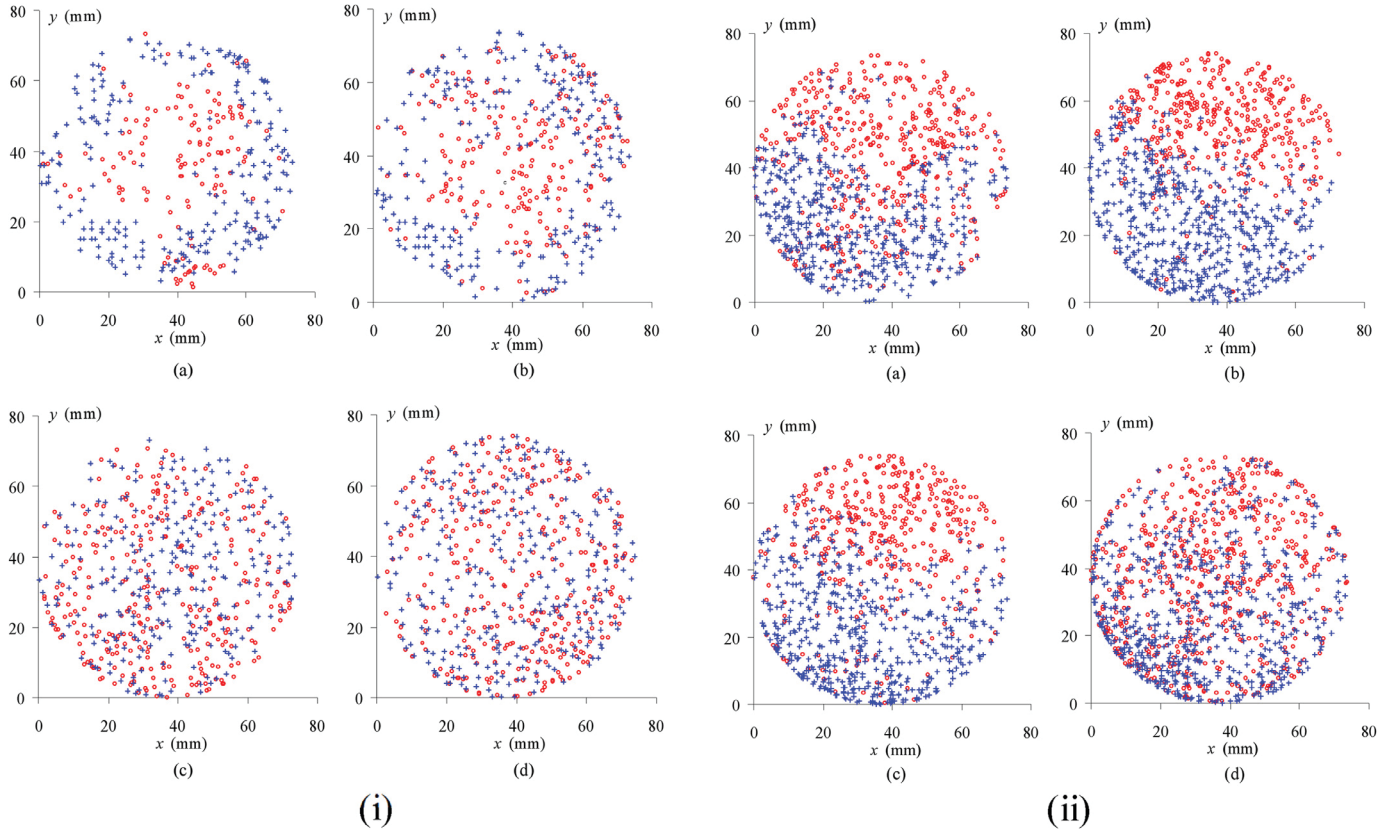

Fig. 7. Projection of trajectories in test sections S_i for $<\alpha_p>=0.30$ a) S_1; b) S_2; c) S_3; d) S_4; in the case of i) aligned case and ii) tilted case. Symbols (o) and (+) indicate the directions (ascending and descending, respectively). $<\alpha_p>=0.3$.

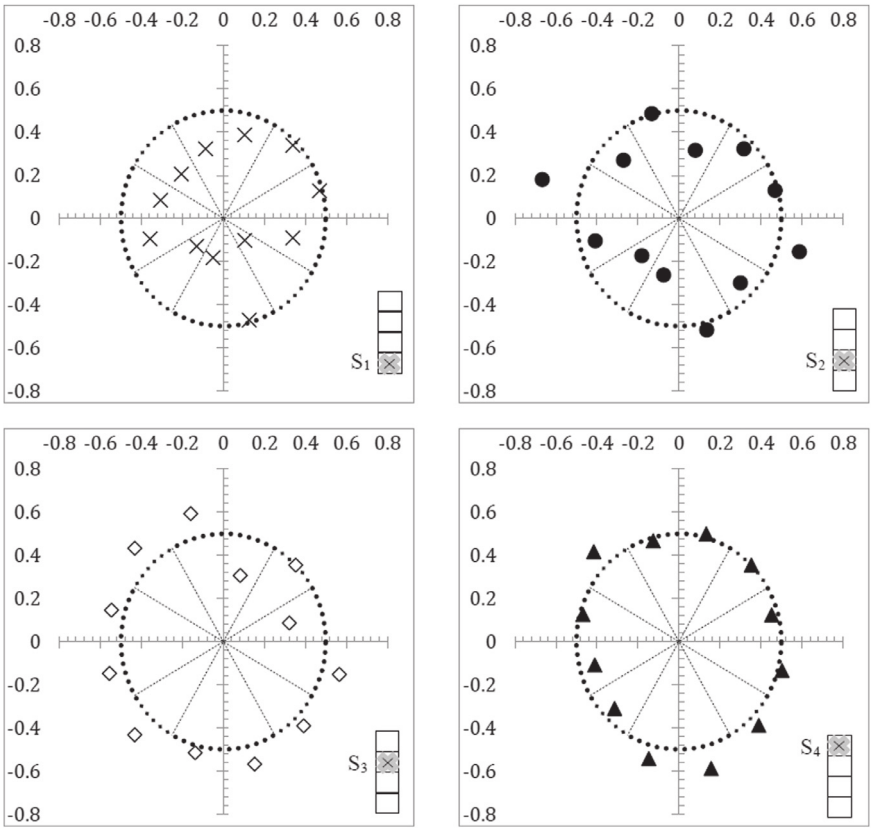

Fig. 8. Homogeneity analysis in terms of particle crossing moving upwards $\varphi_{up,j}$, for different cross sections Si, for the aligned column. $<\alpha_p>=0.3$.

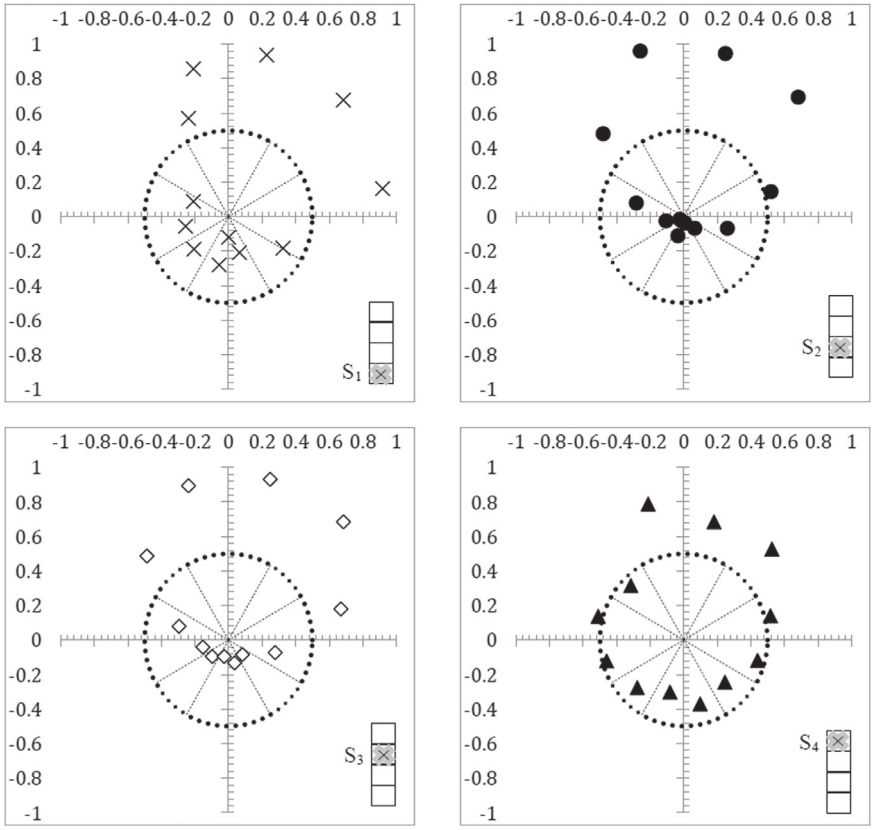

Fig. 9. Homogeneity analysis in terms of particle crossing moving upwards $\varphi_{up,j}$, for different cross sections S_i, for the tilted column.

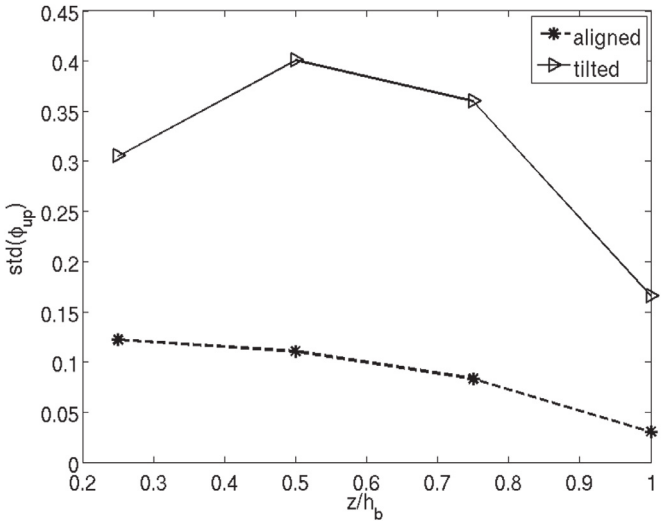

Fig. 10. Evolution of the standard deviation of $\varphi_{up,j}$ as a function of the normalized bed height, z/hb.

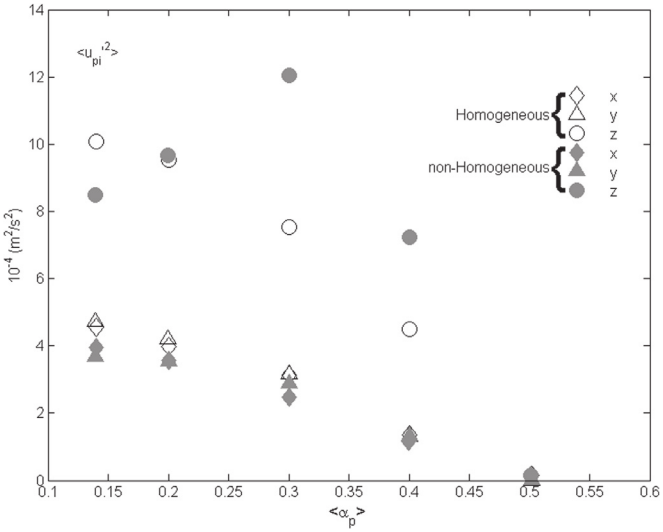

Fig. 11. Variance of particle velocity component as a function of $<\alpha_p>$. Comparison between homogeneous (vertically aligned) and non-homogeneous (tilted column).

The diffusion coefficient in each direction is then given by:

$$D_{ii} = \left\langle u_{pi}^2(t) \right\rangle T_{ii}^L \tag{10}$$

It is then clear from plots of Figs. 11 and 12 that the diffusion in the vertical direction z is stronger than that of the transverse plane (x,y), resulting from both a larger decorrelation time and a larger velocity variance in z-direction than in x and y-directions.

Diffusion coefficients in transverse (D_{xx} and D_{yy}) and vertical (D_{zz}) directions as a function of global solid fraction are plotted in Fig. 13, for both homogeneous and non-homogeneous cases. In both cases as expected, particle diffusion is strongly anisotropic, the diffusion in z-direction being an order of magnitude larger than that in x and y-directions at all solid fractions. In the homogeneous case, the diffusion coefficient is a decreasing function of solid fraction but exhibits a slight maximum around $<\alpha_p> = 0.2$ (open symbols in Fig. 13) for the three components. As for the evolution of particle axial velocity variance with solid fraction (Fig. 11), this maximum is around $<\alpha_p> = 0.3$ in the non-homogeneous case, and maximum differences with the homogeneous case are

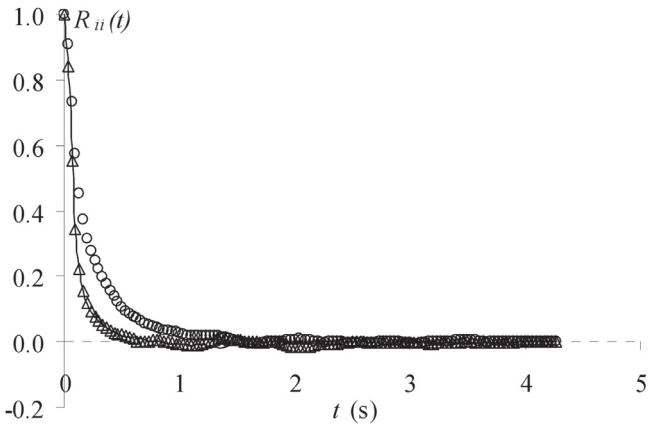

Fig. 12. Particle Lagrangian velocity autocorrelation coefficient versus time for $<\alpha_p>=0.3$. Homogeneous case. (o) z, (Δ) y and (—) x components.

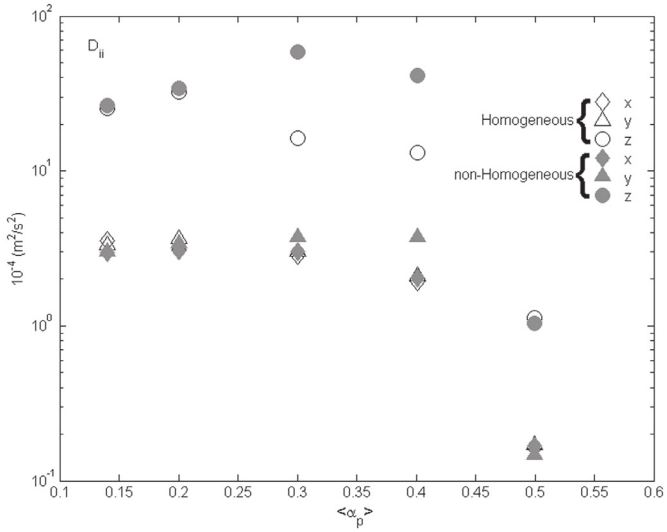

Fig. 13. Particle diffusion coefficient D_{ii} in 3 directions (D_{zz}, D_{yy} and D_{xx}). Comparison between homogeneous (open symbols) and non-homogeneous (filled symbols) cases.

Table 3.
Relative difference δD_{ii} between homogeneous and inhomogeneous cases.

$<\alpha_p>$	δD_{xx}	δD_{yy}	δD_{zz}
0.14	0.17	0.10	−0.05
0.2	0.02	0.06	−0.07
0.3	−0.07	−0.23	−2.62
0.4	−0.07	−0.75	−2.14
0.5	−0.02	0.14	0.07

observed in the same range of $\langle\alpha_p\rangle$, between 0.3 and 0.4. Maximum relative differences are reached for the z-component in that range of concentration, due to the development of a large recirculation pattern evidenced by the trajectories envelope displayed in Fig. 5.

Relative differences $\delta D_{ii} = 1\text{-}D_{iinH}/D_{iiH}$ are reported in Table 3 for all solid fraction investigated. At lower concentration ($<\alpha_p>=0.1$ and 0.2), differences between both cases are not significant in the vertical direction, suggesting that the large-scale coherent structure is not fully developed, probably due to a too small apparent density-induced collective effect. However, at the lowest concentration, the effect of the tilt is to decrease the diffusivity of particles in the horizontal plane. At high concentration ($<\alpha_p>=0.5$), this coherent motion of particles is damped probably due to the bed aspect ratio (height of the bed compares with column diameter in that case) and the differences between the two cases are also negligible. The maximum difference is reached in the range of concentration 0.3–0.4, the diffusion coefficient in z-direction being more than 2 times larger in the non-homogeneous (tilted column) case than in the homogeneous (vertically aligned column) case. Note also that in that range of concentration, the diffusion in the (x,y) plane is not isotropic due to the fact that the plane of inclination is the (y,z) plane, and the relative difference of diffusion coefficient in the y-direction is larger than that observed in the x-direction. In the tilted case, the transverse component variance is very close to the value obtained in the vertical case. It was also shown previously that the velocity fluctuation in the horizontal plane was the correct scaling velocity for collisions (Aguilar-Corona et al., 2011); or in other words, the horizontal fluctuations determined the uncorrelated motion of the particles (not only Gaussian but also Maxwellian, hence isotropic). As a result, tilting the column does not significantly affect the velocity variance (hence the pdf) of the uncorrelated part of particles motion. In return, as shown by our measurements, the diffusive motion in the y-direction is slightly affected by the column tilt. Therefore, the decorrelation time is increased by the tilt due to the small gravity component normal to the wall.

It can be concluded that when a recirculation loop develops in the whole bed volume, it mainly contributes to the increase of particle velocity fluctuations in the vertical direction and also in the decorrelation time, leading to a significant increase of particle diffusivity in that direction. In this range of high particle Reynolds and finite Stokes numbers, the vertical alignment of the fluidisation column is an important criterion regarding the validation of numerical methods in concentrated two-phase flows. The present experiments have been carried out in a liquid fluidized bed where the agitation of fluid, and consequently that of particles, is mainly induced by wake effects (also referred to as pseudo-turbulence). Note that this situation is quite different from gas-solid fluidisation where as general case, particle agitation is driven by the turbulence of the continuous phase, modulated by particle inertia and finite size effects. In the latter case, the effect of a small tilt of the column would probably not be the same, because of the turbulent large-scale induced intense mixing that would prevent the development of coherent structures at the bed scale. Hence, this situation is particular to gravity driven dispersed flow at high concentration for which proper turbulence of the carrying phase remains small compared to that induced by wake effects.

4. Conclusions

In this work, we carried out an experimental investigation of the 3-D particle fluctuating motion in a liquid fluidized bed and compare two different situations: a homogeneous fluidisation regime (homogeneous feeding in the entry section and carefully vertically aligned bed) and a non-homogeneous fluidisation regime resulting from a small tilt (0.3°) of the fluidisation column with the vertical.

The bed expansion is not modified significantly by the tilt, as a result of momentum conservation averaged in the bed volume, which at first order balances the buoyancy force and the drag force based on averaged slip velocity. In turn, we show that the particle trajectories in the bed are strongly modified, shifting from an overall uniformly distributed random motion in the bed with axisymmetric toroidal structure in the bottom part, to large-scale recirculation patterns in a given range of bed expansion (solid fraction). As a consequence, the particle velocity variance and self-diffusion coefficient are significantly affected by the tilt in vertical direction. In particular, it is shown that the change observed on these quan-

tities depends on the fluidisation velocity and that the maximum variation occurs for solid fractions ranging between 0.3 and 0.4. It is also possible, although not investigated in this study, that the particle velocity fluctuations depend also on the particle inertia (Stokes number). These results are relevant when comparisons between experiments and numerical simulations are conducted at an industrial scale. If the experiment is not accurately aligned with the vertical, mixing of passive scalar and/or the transport of mass or heat could be significantly affected by the non-homogeneous state of fluidisation. It is also clear from the results presented in this work that the three dimensional character of the fluctuating motion has to be taken into account when comparing with the numerical simulations and models.

This investigation showed evidence of large sensitivity to very small misalignments with respect to the vertical in fluidized beds. The implications of such an effect are very important when designing a model experiments for the validation of numerical simulations.

Acknowledgements

The authors wish to express their gratitude to the National Science and Technology Council of Mexico (CONACYT) and the research federation FERMaT (FR CNRS 3089) for funding this project.

References

Aguilar, A., 2008. Agitation Des Particules Dans Un Lit Fluidisé liquide. Étude expérimentale Ph.D. thesis. Institut National Polytechnique de Toulouse, France.
Aguilar-Corona, A., Zenit, R., Masbernat, O., 2011. Collisions in a liquid fluidized bed. Int. J. Multiphase Flow 37 (7), 695–705.
Al-Dibouni, M.R., Garside, J., 1979. Particle mixing and classification in liquid fluidized beds. Trans. Inst. Chem. Eng. 57 (2), 94–103.
Anderson, T.B, Jackson, R., 1969. Fluid mechanical description of fluidized beds. Comparison of theory and experiments. Ind. Eng. Chem. Fundam. 8, 137–144.
Buyevich, Y.A., 1994. Fluid dynamics of coarse dispersions. Chem. Eng. Sci. 49 (8), 1217–1228.
Carlos, C.R., Richardson, J.F., 1968. Solids movements in liquid fluidized beds-I Particle velocity distribution. Chem. Eng. Sci. 23 (8), 813–824.
Chaikittisilp, W., Taenumtrakul, T., Boonsuwan, P., Tanthapanichakoon, W., Charinpanitkul, T., 2006. Analysis of solid particle mixing in inclined fluidized beds using DEM simulation. Chem. Eng. J. 122 (1), 21–29.
Del Pozo, M., Briens, C.L., Wild, G., 1992. Effect of column inclination on the performance of three-phase fluidized beds. AIChE J. 38 (8), 1206–1212.
Didwania, AK, Homsy, GM, 1981. Flow regime and flow transitions in liquid-fluidized beds. Int. J. Multiphase Flow 7, 563–580.
Di Felice, R., 1995. Hydrodynamics of liquid fluidisation. Chem. Eng. Sci. 50 (8), 1213–1245.
Dorgelo, E.A.H., Van Der Meer, A.P., Wesselingh, J.A., 1985. Measurement of the axial dispersion of particles in a liquid fluidized bed applying a random walk method. Chem. Eng. Sci. 40 (11), 2105–2111.
Duru, P., Guazzelli, É., 2002. Experimental investigation on the secondary instability of liquid-fluidized beds and the formation of bubbles. J. Fluid Mech. 470, 359–382.
El-Kaissy, M.M., Homsy, G.M., 1976. Instability waves and the origin of bubbles in fluidized beds. Int. J. Multiphase Flow 2-4, 379–395.
Gordon, L.J., 1963. Solids Motion in a Liquid Fluidized Bed PhD thesis. University of Washington.
Handley, D., Doraisamy, A., Butcher, K.L., Franklin, N.L., 1966. A study of the fluid and particle mechanics in liquid-fluidized beds. Trans. Inst. Chem. Eng. 44, T260–T273.
Hassan, A.Y., Dominguez-Ontiveros, E.E., 2008. Flow visualization in a pebble bed reactor experiment using PIV and refractive index matching techniques. Nucl. Eng. Des. 238 (11), 3080–3085.
Homsy, G.M., 1998. Nonlinear waves and the origin of bubbles in fluidized beds. App. Sci. Res. 58 (1), 251–274.
Homsy, G.M., El-Kaissy, M.M., Didwania, A., 1980. Instability waves and the origin of bubbles in fluidized beds - II. Int. J. Multiphase Flow 6, 305–318.
Hudson, C., Briens, C.L., Prakash, A., 1996. Effect of inclination on liquid-solid fluidized beds. Powder Tech. 89 (2), 101–113.
Juma, A.K.A., Richardson, J.F., 1983. Segregation and mixing in liquid fluidized beds. Chem. Eng. Sci. 38 (6), 955–967.
Kang, Y., Nah, J.B., Min, B.T., Kim, S.D., 1990. Dispersion and fluctuation of fluidized particles in a liquid-solid fluidized bed. Chem. Eng. Comm. 97 (1), 197–208.
Kennedy S., C., Bretton R., H., 1966. Axial dispersion of spheres fluidized with liquids. AIChE J. 12 (1), 24–30.
Latif, B.A.J., Richardson, J.F., 1972. Circulation patterns and velocity distribution for particles in a liquid fluidized bed. Chem. Eng. Sci. 27, 1933–1949.
Sundaresan, S., 2003. Instabilities in fluidized beds. Annu. Rev. Fluid Mech 35 (1), 63–88.
Valverde, J.M., Castellanos, A., Quintanilla, M.A.S., Gilabert, F.A., 2008. Effect of inclination on gas-fluidized beds of fine cohesive powders. Powder Tech. 182 (3), 398–405.
Van Der Meer, A.P., Blanchard, C.M.R.J.P., Wesselingh, J.A., 1984. Mixing of particles in liquid fluidized beds. Chem. Eng. Res. Des. 62, 214–222.
Willus, C.A., 1970. An Experimental Investigation of Particle Motion in Liquid Fluidized Bed. Thesis of California Institute of Technology, United States of America.
Yakubov, B., Tanny, J., Maron, D.M., Brauner, N., 2005. The effect of pipe inclination on a liquid-solid fluidized bed. HAIT J. Sci. Eng. B 3, 1–19.
Yamazaki, R., Sugioka, R., Ando, O., Jimbo, G., 1989. Minimum velocity for fluidisation of an inclined fluidized bed. Kagaku Kogaku Ronbunshu 15 (2), 219–225.
Yutani, N., Ototake, N., Too, J.R., Fan, L.T., 1982. Estimation of the particle diffusivity in a liquid-solids fluidized bed based on a stochastic model. Chem. Eng. Sci. 37 (7), 1079–1085.
Zenit, R., Tsang, Y.H., Koch, D.L., Sangani, A.S., 2004. Shear flow of a suspension of bubbles rising in an inclined channel. J. Fluid Mech. 515, 261–292.